The American Journal of Pathology, Vol. 185, No. 8, August 2015

The American Journal of
PATHOLOGY
ajp.amjpathol.org

CARDIOVASCULAR, PULMONARY, AND RENAL PATHOLOGY

Activation of Autophagy and Nucleotide-Binding Domain Leucine-Rich Repeat–Containing-Like Receptor Family, Pyrin Domain–Containing 3 Inflammasome during *Leishmania infantum*–Associated Glomerulonephritis

Kevin J. Esch,* Robert G. Schaut,† Ian M. Lamb,† Gwendolyn Clay,‡ Ádila L. Morais Lima,§ Paulo R.P. do Nascimento,§ Elizabeth M. Whitley,* Selma M.B. Jeronimo,§ Fayyaz S. Sutterwala,‡ Joseph S. Haynes,* and Christine A. Petersen*†

From the Department of Veterinary Pathology, College of Veterinary Medicine, Iowa State University, Ames, Iowa; the Department of Epidemiology,† College of Public Health, University of Iowa, Iowa City, Iowa; the Inflammation Program,‡ Department of Internal Medicine, University of Iowa Carver College of Medicine, Iowa City, Iowa; and the Department of Biochemistry,§ Institute of Tropical Medicine, Federal University of Rio Grande do Norte, Natal, Brazil*

Accepted for publication April 16, 2015.

Address correspondence to Christine A. Petersen, D.V.M., Ph.D., Department of Epidemiology, Iowa State University, 145 N Riverside Dr, S429 CPHB, Iowa City, IA 52241. E-mail: christine-petersen@uiowa.edu.

Chronic kidney disease is a major contributor to human and companion animal morbidity and mortality. Renal complications are sequelae of canine and human visceral leishmaniasis (VL). Despite the high incidence of infection-mediated glomerulonephritis, little is known about pathogenesis of VL-associated renal disease. *Leishmania infantum*–infected dogs are a naturally occurring model of VL-associated glomerulonephritis. Membranoproliferative glomerulonephritis type I [24 of 25 (96%)], with interstitial lymphoplasmacytic nephritis [23 of 25 (92%)], and glomerular and interstitial fibrosis [12 of 25 (48%)] were predominant lesions. An ultrastructural evaluation of glomeruli from animals with VL identified mesangial cell proliferation and interposition. Immunohistochemistry demonstrated significant *Leishmania* antigen, IgG, and C3b deposition in VL dog glomeruli. Asymptomatic and symptomatic dogs had increased glomerular nucleotide-binding domain leucine-rich repeat–containing-like receptor family, pyrin domain containing 3 and autophagosome-associated microtubule-associated protein 1 light chain 3 associated with glomerular lesion severity. Transcriptional analyses from symptomatic dogs confirmed induction of autophagy and inflammasome genes within glomeruli and tubules. On the basis of temporal VL staging, glomerulonephritis was initiated by IgG and complement deposition. This deposition preceded presence of nucleotide-binding domain leucine-rich repeat–containing-like receptor family, pyrin domain containing 3–associated inflammasomes and increased light chain 3 puncta indicative of autophagosomes in glomeruli from dogs with clinical VL and renal failure. These findings indicate potential roles for inflammasome complexes in glomerular damage during VL and autophagy in ensuing cellular responses. *(Am J Pathol 2015, 185: 2105–2117; http://dx.doi.org/10.1016/j.ajpath.2015.04.017)*

Renal disease due to glomerulonephritis and interstitial nephritis is a complication of visceral leishmaniasis (VL), occurring in >96% of symptomatic dogs and 25% to 51% of human cases.[1–4] Alterations in renal function during active VL in both dogs and humans are usually reversible with prompt anti-*Leishmania* therapy.[5,6] However, VL-associated kidney disease is progressive and, without therapy, can result in end-stage renal disease (ESRD; approximately 1.5% of human cases).[4] Previous reports regarding the pathophysiology of VL-associated renal disease are conflicting, showing either presence or absence of IgG and complement protein C3.[1,7] Accurate assessment of VL-associated glomerular lesions early in their progression is essential

Supported in part by National Institutes of Allergy and Infectious Diseases (NIH) grant AI088051 (C.A.P.) and NIH grant R01 AI087630 (F.S.S.).

Disclosures: K.J.E. was supported by Pfizer Animal Health-MAF Veterinary Fellowship for Advanced Study grant D09CA-911, supported by Pfizer Animal Health.

http://dx.doi.org/10.1016/j.ajpath.2015.04.017

to determining an efficacious treatment regimen and aid in determining prognosis.

Membranoproliferative glomerulonephritis (MPGN) is traditionally classified as type I, II, or III on the basis of location and character of protein deposits.[8] These characterizations are based on morphology, rather than specific cause, and a spectrum of changes can often be found within a single biopsy specimen. Recent efforts to reclassify MPGN by pathogenesis are better predictors of clinical outcome and may help target therapy. The new classification scheme uses immunofluorescence or immunohistochemistry to define lesions as immune-complex MPGN (with IgG, IgM, and/or complement), as Ig-negative C3 glomerulopathy, or dense deposit disease.[8,9] Podocytes, versatile, long-lived cells constructing the glomerular filtration slit, and mesangial cells, a major resident phagocyte within the glomerular mesangium, play definitive roles in MPGN. The reaction of mesangial cells, ultrastructural changes, and apoptosis of glomerular podocytes are the basis for traditional MPGN classification. The mechanisms through which the glomerular apparatus (podocytes, mesangial cells, and endothelial cells) responds to inflammatory stimuli are not well understood. Multiple reports have demonstrated the importance of autophagy in glomerular basement membrane (GBM) maintenance as a normal function of podocytes.[10–13] Podocyte-specific knockout of light chain 3 (LC3), an autophagy protein, resulted in glomerulosclerosis with accumulation of polyubiquitinated proteins by 24 months.[10] Renal elevations in LC3 were identified in response to increased glucose in a model of diabetic nephropathy, and in patients with Fabry disease.[14,15] Regulation of renal fibrosis and the clearance of immune complexes during inflammatory MPGN are potentially regulated through autophagy-associated pathways.

Inflammasomes are protein complexes that respond to a variety of cellular stressors and direct receptor-ligand interactions.[16] The nucleotide-binding domain leucine-rich repeat–containing-like receptor family, pyrin domain containing 3 (NLRP3) inflammasome is well characterized and responds to both pathogen-associated molecular patterns and stress-related molecules.[16] The NLRP3 inflammasome complex is composed of NLRP3, the adaptor molecule apoptosis-associated speck-like protein containing a caspase activation and recruitment domain (ASC), and the cysteine protease caspase-1. NLRP3 responds to a wide array of structurally and chemically diverse agonists, including single- and double-stranded bacterial RNA, ATP, urate crystals, silica, and bacterial pore-forming toxins.[17,18] In the kidney, inflammasome products IL-1β and IL-18 are key mediators of renal disease.[19] Activation of NLRP3-mediated glomerular injury has been shown to be stimulated by NADPH oxidase activation.[20] This process was recently associated with ASC, a major inflammasome adapter protein, in obesity-induced glomerulonephritis.[21] Immune-complex deposition within the subendothelial space and within the glomerular mesangium may drive proinflammatory podocyte and filtration apparatus injury through activation of ASC and NLRP3.

Herein, we examined mechanisms that may mediate or be sequelae of MPGN during VL. Glomerulonephritis associated with *Leishmania infantum* infection was present in both symptomatic and asymptomatic disease and was primarily membranoproliferative, with subendothelial and mesangial electron-dense deposits and endocapillary and mesangial cell hypertrophy. We clearly demonstrated that protein deposits during VL-associated MPGN were composed of *L. infantum* antigen, IgG, and complement protein C3. This study is the first to evaluate glomerular autophagy and NLRP3 inflammasome presence associated with VL clinical stage in the renal glomerulus. These data suggest that inflammasome engagement and LC3-dependent macroautophagy may contribute to the pathogenesis of immune complex–mediated renal disease and VL-associated MPGN.

Materials and Methods

Animals

Animals were staged before necropsy on the basis of clinical presentation, including lymphadenopathy, palpable liver or spleen, and skin lesions typical of VL. Fifteen dogs from the United States were evaluated via full physical examination and fecal examination for comorbidities. The 10 dogs from Brazil, evaluated via full physical examination, were more likely to be symptomatic at the time of presentation (7 of 10 dogs), and also had a higher probability of comorbidities, including malnutrition, helminth infection, or rickettsial infections, and had positive anti-*Leishmania* antibodies. Study animals were enrolled for this study on the basis of immunofluorescence antibody test serology, as previously described,[22] and were euthanized with owner's consent. Necropsies were performed by pathologists (K.J.E., J.S.H.) at Iowa State University (Ames, IA) College of Veterinary Medicine and at UFRN (Natal, Brazil). Full or partial necropsies were performed on each animal, with gross evaluation and tissues harvested for histopathological examination. These studies were approved by the Institutional Animal Care and Use Committee at Iowa State University and the Animal Research Ethics Committee of Federal University of Rio Grande do Norte (CEUA-UFRN; Natal, Brazil).

Histopathology

Tissues were fixed in 10% neutral-buffered formalin, paraffin embedded, and processed for routine histopathological evaluation. Sections (3 μm thick) were stained with hematoxylin and eosin, Masson's trichrome, or periodic acid– Schiff–methenamine silver. The sections were analyzed by light microscopy (model BX41; Olympus, Center Valley, PA), and renal changes were classified according to World Health Organization criteria for morphological classification glomerulonephritis. Lesions were scored from grade 1 to 4 on the basis of expansion of the mesangium, mesangial fibrosis, thickening of capillary

loops, periglomerular inflammation, and percentage of sclerotic glomeruli. All sections were evaluated by a trained veterinary pathologist (K.J.E., J.S.H.).

Electron Microscopy

Renal tissue was fixed in 2.0% glutaraldehyde in 0.1 mol/L phosphate buffer, pH 7.4. Ultrathin sections were stained for analysis by transmission electron microscopy. Tissue fragments (1 mm) were fixed in 2.5% glutaraldehyde in 0.1 mol/L sodium cacodylate buffer. After fixation, samples were rinsed in cacodylate buffer, post-fixed in 2% osmium tetroxide, dehydrated in alcohols, cleared in propylene oxide, and embedded in Eponate 12 epoxy resin (PELCO, Redding, CA). Ultrathin sections were cut, stained with uranyl acetate and lead citrate, and examined with a Tecnai 12 G^2 electron microscope (FEI, Hillsboro, OR).

Immunohistochemistry

Formalin-fixed, paraffin-embedded sections (3 μm thick) were labeled with the following: canine anti-*L. infantum* (hyperimmune serum, 1:500 dilution), anti-canine IgG (2 mg/mL, 1:6000 dilution; Immunovision, Springdale, AZ), anti-canine IgM (2 mg/mL, 1:2000; Immunovision), anti-canine C3b (1 mg/mL, 1:200 dilution; Bethyl Labs, Montgomery, TX). For IgG and IgM labeling, slides were preheated to 57°C for 30 minutes before deparaffinization. Endogenous peroxidases were inhibited by addition of 3% H_2O_2, followed by a rinse in ultrapure water. Samples were blocked with 10% normal goat serum in phosphate-buffered saline. Samples were stained with multilink (Biogenex, Fremont, CA) and developed with Streptavidin horseradish peroxidase and Nova Red (Vectorlabs, Burlingame, CA) before counterstaining with hematoxylin. Labeling for *Leishmania* antigen was performed as previously published.[23] Appropriate controls were included in each experiment.

Immunofluorescence

Formalin-fixed, paraffin-embedded sections and cryosections were labeled with 0.2 mg/mL polyclonal canine cross-reactive anti-human LC3 (1:50 dilution; AbCam, Cambridge, MA) and 0.5 mg/mL polyclonal canine cross-reactive anti-human NLRP3 (1:100 dilution; AbCam). Sections were washed and cryosections were fixed with acetone for 5 minutes, then air dried for 30 minutes. Sections were then permeabilized, washed, and treated with blocking immunofluorescence buffer before labeling with primary antibodies. Secondary antibodies for LC3 (Texas Red—conjugated anti-rabbit IgG) and NLRP3 (Alexa Fluor 400—conjugated anti-goat IgG) were used at a concentration of 2 βg/mL. Coverslips were added using Prolong Gold Anti-Fading Reagent (Life Technologies, Grand Island, NY) and were analyzed via confocal microscopy. Secondary antibody only and unstained controls were included for each experiment.

Image Analysis

A threshold of positivity was generated using color threshold analysis (ImageJ version 1.48; NIH, Bethesda, MD; *http://imagej.nih.gov/ij*), and immunohistochemical positivity was quantified as area of immunohistochemical-positive staining as a percentage of total glomerular area. For immunofluorescence, glomeruli were imaged individually and analyzed with ImageJ using threshold analysis to calculate percentage of glomerular area with positive labeling, the number of positive cells as a percentage of total glomerular cells was counted as DAPI-positive nuclei in fluorescent images, and density of positive labeling was determined.

L. infantum Mouse Infection Model

The Institutional Animal Care and Use Committee at the University of Iowa (Iowa City, IA) approved all mouse protocols used in this study. The generation of $Asc^{-/-}$ mice has been previously described.[24] Wild-type (WT) C57BL/6N and $Asc^{-/-}$ mice were infected via i.v. injection into the tail vein of 10^6 *L. infantum* metacyclic promastigotes. Mice were euthanized 4 weeks after infection, and necropsy was performed in a laminar flow hood. Tissues were collected in 10% neutral-buffered formalin, embedded in Tissue-Tek OCT (Sakura-Finetek USA, Torrance, CA), and frozen as cryosections, or collected in 2.0% glutaraldehyde in 0.1 mol/L phosphate buffer (pH 7.4) for transmission electron microscopy, as described. Renal sections were evaluated as described for the dog. No mice in any group had identifiable gross lesions. Overall parasite burdens at 4 weeks after infection, calculated via real-time quantitative PCR (qPCR) on spleen and liver tissues, were highly variable, making statistical evaluation of parasite burden between $Asc^{-/-}$ and WT mice uninformative (data not shown).

RNA Isolation, Reverse Transcription, and PCR from Renal Tissue

RNA was isolated via chloroform and column extraction.[25] RNase Out (Life Technologies, Carlsbad, CA) was added to avoid RNase-mediated RNA degradation. Samples were quantified via ND-1000 (Thermo Scientific, Wilmington, DE) to standardize all samples to 200 ng of total RNA per reverse transcription reaction. An iScript cDNA synthesis kit (Bio-Rad, Hercules, CA) was used per manufacturer's protocol. Reverse transcription was performed in a Vapoprotect thermocycler (Eppendorf, Enfield, CT): 5 minutes at 25°C, 6 minutes at 42°C, 5 minutes at 72°C, and held at 4°C. Primers were designed using the Primer-BLAST Tool (National Center for Biotechnology Information) with the *Canis lupus familiaris* genome for reference. iTaq Universal SYBR Green Supermix (Bio-Rad) was used for the qPCR with mastermix of primer sets generated. Primers were used at a final concentration of 500

Table 1 Primers Used for qPCR

Gene name	Primer sequence	RNA accession no./reference
Atg7	Forward: 5′-GGCGGAGGCACCAAATGAT-3′	XM_005632154.1
	Reverse: 5′-CCACATCCAAGGCACTGCTA-3′	
Lc3	Forward: 5′-CGGTACAAGGGTGAGAAGCA-3′	XM_536756.3
	Reverse: 5′-GAGCTGTAAGCGCCTCCTAAT-3′	
Pycard	Forward: 5′-GAGACCTCACACAAAGGCCA-3′	XM_001003125.1
	Reverse: 5′-TGCTGGTCCACAAAGTGTGA-3′	
Casp1	Forward: 5′-GGCTGTTTGTCCGGTCAGTA-3′	NM_001003125.1
	Reverse: 5′-CCTCGTGGTTCAGCACTCTT-3′	
Nlrp3	Forward: 5′-ACAACAGGGCTGCATCCTAC-3′	XM_005623150.1
	Reverse: 5′-AGACAATGGTCAGCTCAGGC-3′	
Gapdh	Forward: 5′-CATTGCCCTCAATGACCACT-3′	Maeda et al[27]
	Reverse: 5′-TCCTTGGAGGCCATGTAGAC-3′	

Primers were obtained using the Primer-BLAST tool on the National Center for Biotechnology Information website (*http://www.ncbi.nlm.nih.gov/tools/primer-blast*).

Atg7, autophagy-related 7; *Casp1*, IL-1 converting enzyme; *Gapdh*, glyceraldehyde-3-phosphate dehydrogenase; *Lc3*, microtubule-associated protein 1 light chain 3β; *Nlrp3*, nucleotide-binding domain leucine-rich repeat–containing-like receptor family, pyrin domain containing 3; *Pycard*, N-terminal PYRIN-PAAD-DAPIN domain and a C-terminal caspase-recruitment domain; qPCR, real-time quantitative PCR.

nmol/L per well reaction. An ABI 7000 qPCR machine (Applied Biosystems, Carlsbad, CA) was used. Amplification conditions for all genes were the same: 5 minutes at 95°C, 40 cycles of 15 seconds at 95°C, and 1 minute at 60°C (measure fluorescence step) and a dissociation step of 15 seconds at 95°C, 1 minute at 60°C, 15 seconds at 95°C, and 15 seconds at 60°C. C_T values were generated using ABI PRISM SDS Software version 1.2.3 (Applied Biosystems). C_T values were calculated and normalized to endogenous control (glyceraldehyde-3-phosphate dehydrogenase) and expressed relative to control dogs using the $2^{-\Delta\Delta C_T}$ method.[26] Primers are listed in Table 1.

LCM

Archived cryosections were stained with nuclease-free hematoxylin [laser-capture microdissection (LCM) frozen section staining kit, Arcturus Histogene; Applied Biosystems] in ultrapure, nuclease-free water. Sections were dehydrated in alcohol and xylene and prepared for LCM, as previously described.[28] Slides were evaluated by a trained pathologist; glomerular tufts, renal proximal tubular epithelium, and renal interstitial regions were excised separately for compartmental expression analysis. Cells were collected onto LCM caps (Capsure; Applied Biosystems) and submerged in 50 βL Tri Reagent (Sigma-Aldrich, St. Louis, MO), and caps were removed by centrifugation. Cells were frozen at −80°C until further processing. RNA extraction, reverse transcription, and qPCR were performed as described above.

Western Blot Analysis

Cryosections (20 μm thick) were isolated from OCT-embedded dog kidney samples on a cryostat. The cryosections were placed into a mixture of NP-40 lysis buffer and 1× Halt Protease & Phosphatase Inhibitor Cocktail (Thermo Fisher Scientific, Waltham, MA). The protein concentration of each sample was determined by BCA protein assay kit, according to the manufacturer's instructions (Thermo Fisher Scientific). Lysates were normalized to 5 ng protein per sample, and an equal volume of Laemmli running buffer (1:1 ratio) with 5% β-mercaptoethanol was added. The ASC (anti-mouse/human; AdipoGen, San Diego, CA), NLRP3 (mouse IgG2b anti-mouse/human; AdipoGen), and IL-1β (rabbit polyclonal Ig; Abbiotec, San Diego, CA) were diluted 1:1000 in 5% milk in Tris-buffered saline with 0.05% Tween 20. The secondary antibodies for ASC and IL-1β [Goat Anti-Rabbit IgG (H + L); Jackson Immunoresearch, West Grove, PA] and NLRP3 [Rabbit Anti-Mouse IgG (H + L)-horseradish peroxidase; Southern Biotech, Birmingham, AL] were diluted 1:1000 in

Table 2 Microscopic Lesions during VL-Associated Glomerulopathy

Variable	Asymptomatic	Symptomatic	All VL dogs
Mesangial proliferation	92.31 (12/13)	100.00 (12/12)	96.00 (24/25)
Interstitial nephritis	92.31 (12/13)	91.67 (11/12)	92.00 (23/25)
Glomerular hypersegmentation	92.31 (12/13)	100.00 (12/12)	96.00 (24/25)
Glomerular and interstitial fibrosis	7.69 (1/13)	91.67 (11/12)*	46.00 (12/25)
Double-contour GBM	15.38 (2/13)	91.67 (11/12)*	52.00 (13/25)

Data are given as percentage (number/total).

*$P < 0.001$ from asymptomatic group.

GBM, glomerular basement membrane; VL, visceral leishmaniasis.

Tris-buffered saline with 0.05% Tween 20. SuperSignal West Femto Chemiluminescent Substrate (500 μL; Thermo Fisher Scientific) was added to each membrane; membranes were subsequently imaged by a LI-COR Odyssey (LI-COR Biosciences, Lincoln, NE). Next, membranes were probed for β-actin using an anti−β-actin antibody (mouse monoclonal AC-15; Ambion of Life Technologies, Madison, WI) and a rabbit anti-mouse IgG (H + L)-horseradish peroxidase secondary antibody (Southern Biotech). Quantification of the images obtained was performed using ImageJ software version 1.48 (NIH, Bethesda, MD; *http://imagej.nih.gov/ij*).

Enzyme-Linked Immunosorbent Assay

Serum samples from four control and four naturally infected dogs were collected from whole blood. As positive control, peripheral blood mononuclear cells were stimulated with lipopolysaccharide for 24 hours, and their lysates were collected. The Canine IL-1β VetSet ELISA Development Kit (Kingfisher Biotech Inc., Saint Paul, MN) was used for all samples, according to the manufacturer's instructions. Absorbance was measured at 450 nm by a VERSAMAX microplate reader (Molecular Devices, Sunnyvale, CA). Quantification was performed using Microsoft Excel (Redmond, WA).

Statistical Analysis

Statistical analysis was conducted with pair-wise *t*-tests or one-way analysis of variance with Tukey post test, as appropriate (Graph Pad Prism version 5; GraphPad Software, La Jolla, CA); statistical significance was set at $\alpha = 0.05$. One-way analysis of variance was also performed to demonstrate statistically significant fold changes in transcription data between control and experimental groups.

Results

VL-Associated Glomerulopathy Lesions Are Present in Asymptomatic Animals, with GBM Expansion and Fibrosis Associated with Symptomatic Disease

To assess the onset of glomerular lesions and their association with symptomatic VL, we evaluated renal samples from 13 asymptomatic and 12 symptomatic dogs infected with *L. infantum*, and kidneys from five control (noninfected) dogs that presented to Iowa State University Department of Veterinary Pathology. Predominant microscopic lesions in common to symptomatic and asymptomatic dogs were mesangial hypercellularity (96%; 24 of 25 total cases), glomerular hypersegmentation (96%; 24 of 25 total cases), and interstitial nephritis, characterized by infiltration of macrophages, lymphocytes, and plasma cells into periglomerular and perivascular areas (92%; 23 of 25 total cases) (Table 2 and Figure 1, A and B). Factors predictive of symptomatic disease were irreversible lesions typically associated with chronicity. Glomerular and interstitial fibrosis significantly increased within the symptomatic group (91.67%; 11 of 12 cases) compared with the asymptomatic group (7.69%; 1 of 13 cases) (Table 2 and Figure 1, C and D). Trichrome-positive collagen, evaluated with color-threshold image analysis,

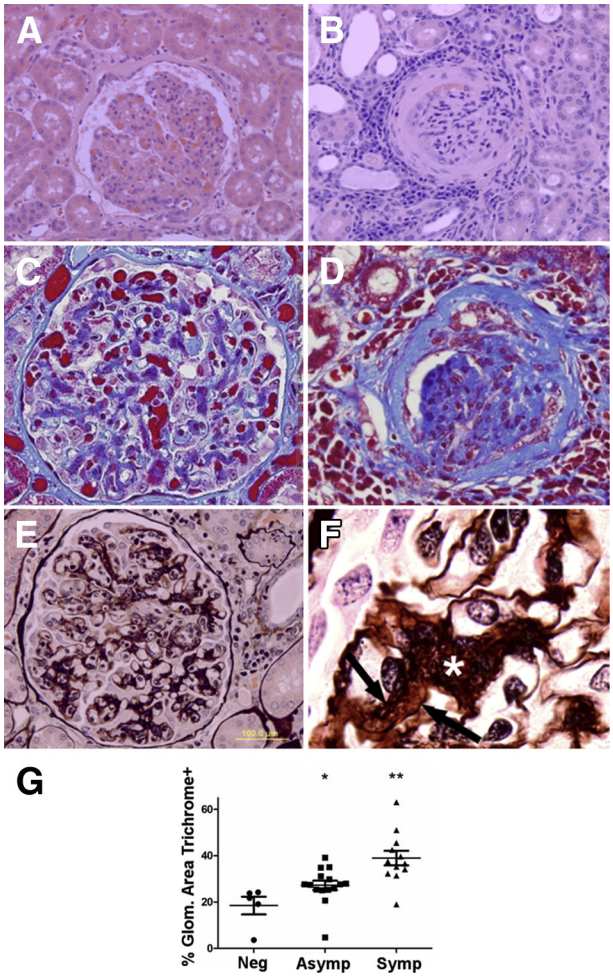

Figure 1 Visceral leishmaniasis (VL)—associated glomerular lesions are present in asymptomatic dogs, with glomerular fibrosis in symptomatic VL animals. **A:** Asymptomatic VL. Glomeruli have diffuse mesangial and endocapillary hypercellularity with glomerular tuft hypersegmentation and segmental thickening of Bowman capsule. Hematoxylin and eosin was used. **B:** Symptomatic VL. Multiple renal glomeruli are sclerotic or contain segmental synechiae, with prominent lymphoplasmacytic and histiocytic interstitial nephritis and fibrosis of Bowman capsule and glomerular tuft. Hematoxylin and eosin was used. **C** and **D:** Trichrome staining identifies progressively increased collagen (blue) within the mesangium of asymptomatic dogs (**C**) and throughout the glomerular tuft and Bowman capsule with synechiae and glomerulosclerosis in symptomatic dogs (**D**). Masson's trichrome was used. **E:** Symptomatic dog glomeruli have robust mesangial expansion, mesangial cell hypercellularity, and interposition. Glomerular basement membranes often are split, with double contours. Periodic acid—Schiff—methenamine silver was used. **F:** Mesangial cell interposition and mesangium expansion (**asterisk**), with double contours because of segmental splitting of the glomerular basement membranes (**arrows**). Periodic acid—Schiff—methenamine silver was used. **G:** Glomerular area positive for collagen is significantly increased with progression of VL. Percentage glomerular (Glom.) area collagen positive in normal controls, asymptomatic (Asymp) VL, and symptomatic (Symp) VL, gated via color-threshold analysis in ImageJ version 1.48. SEM analysis was conducted via one-way analysis of variance with Tukey post test. $^*P < 0.05$, $^{**}P < 0.01$. Original magnifications: ×400 (**A**—**E**); ×1000 (**F**). Neg, negative.

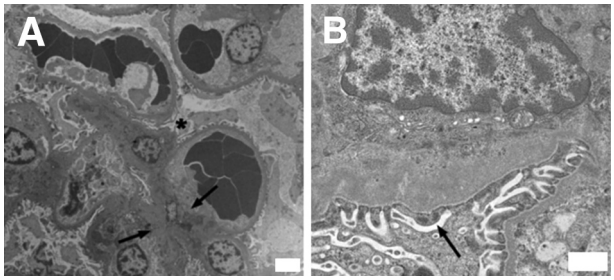

Figure 2 Ultrastructural lesions of visceral leishmaniasis (VL)–associated glomerulonephritis are type I membranoproliferative glomerulonephritis. Renal cortical sections harvested from symptomatic VL dogs. Renal tissue was analyzed via transmission electron microscopy. **A:** Glomerular section with mesangial cell hypercellularity and capillary interposition (**asterisk**). Prominent mesangial and subendothelial deposits (**arrows**). **B:** Prominent subendothelial deposits within glomerular capillary, segmental thickening of glomerular basement membrane. Deposits associated with mild to moderate blunting and fusion of podocyte foot processes (**arrow**) with microvillous transformation. Representative of glomerular lesions from five VL dogs. Original magnifications: ×4320 (**A**); ×27,600 (**B**).

increased in both the asymptomatic and symptomatic animals, and symptomatic dogs had significantly greater staining of collagen than asymptomatic dogs (Figure 1, C, D, and G).

The degree of glomerular fibrosis was closely associated with the clinical status of *L. infantum*–infected dogs. Expansion of mesangial matrix with mesangial cell interposition (Figure 1, E and F) and segmental splitting of the GBM (Figure 1F), analyzed via periodic acid–Schiff–methenamine silver stain, significantly increased within the symptomatic group (91.67%; 11 of 12 cases) compared with the asymptomatic group (15.38%; 2 of 13 cases) (Table 2). Although mesangial cellularity and glomerular hypersegmentation were present during both asymptomatic and symptomatic VL, lesions of chronicity, particularly expansion of mesangium by collagen, were associated with symptomatic VL.

Previous reports of VL-associated glomerulonephritis identify lesions ranging from mesangial proliferative in nature to ESRD with glomerulosclerosis.[1,2,5,7,29,30] Ultrastructural changes evident in glomeruli with early-stage lesions were focal to segmental subendothelial, intramembranous, and/or mesangial, electron-dense deposits, with blunting and fusion of podocyte foot processes. Mesangial cell hypercellularity and interposition were found in symptomatic VL dogs (Figure 2A), with subendothelial and mesangial electron-dense deposits (Figure 2). Endothelial cell hypertrophy and endothelial separation from the GBM were pronounced in all cases. There was moderate microvillous transformation of podocytes with blunting and fusion of podocyte foot processes in symptomatic dogs (Figure 2B). These lesions are consistent with type I MPGN. Accurate characterization of glomerular lesions is becoming increasingly important, on the basis of the emerging goal of individualized therapy. Accurate typing is also prognostically valuable, with a documented fivefold reduction in ESRD on the basis of the extent of GBM and mesangial deposits and the severity of the glomerular lesions.

GBM Deposits Are Associated with Complexes Primarily Composed of *Leishmania* Antigen, IgG, Complement Protein C3b, and Increased Collagen

New efforts to correlate MPGN classification with clinical severity and therapeutic outcome led to glomerular lesions reclassification on the basis of not only location of electron-dense deposits, but also on components within deposits.[8] Previous results regarding deposit components consistently demonstrated presence of *Leishmania* antigen, but are in conflict regarding other mechanistic components (in one case indicating absence of complement, IgG, or IgM, and in another demonstrating presence of IgG, IgM, and complement protein C3).[7,29] Symptomatic and asymptomatic *L. infantum*–infected dogs had significant GBM aggregates of *Leishmania* antigen compared with control animals (Figure 3, A and C). IgG, as a percentage of glomerular area, was also significantly elevated in both asymptomatic and symptomatic VL groups compared with controls (Figure 3, B and D). This finding is consistent with increased γ globulins in dogs with leishmaniasis. There was no difference in IgM within the glomerulus between asymptomatic, symptomatic, or control dogs (data not shown). Immunohistochemical labeling of complement protein C3b was increased in both asymptomatic and symptomatic dogs compared with control (Figure 3E). Although it is not surprising to find IgG-antigen deposits in symptomatic animals, IgG and *L. infantum* antigen deposits were also present in asymptomatic dogs, suggesting immune complex deposition before the onset of symptomatic VL.

Increased NLRP3 Is Associated with Clinical Disease and Glomerular Inflammation

Glomerular immune complex deposition and subsequent impairment of the glomerular filtration apparatus have been previously associated with numerous proinflammatory cytokines, including IL-1β with fibrosis stimulated by transforming growth factor-β.[20,31] Previous reports of VL-associated glomerulonephritis demonstrated increased expression of the adhesion molecules, such as intercellular adhesion molecules and p-selectin.[7] Numerous stimuli can result in NLRP3 inflammasome activation in renal tubular epithelium, including uric acid crystals, amyloid, cholesterol crystals, and high glucose concentrations.[32–34] To evaluate the possible association of inflammasome protein NLRP3 with the progression of VL-associated MPGN, we labeled formalin-fixed, paraffin-embedded sections (Figure 4D) and cryosections (Figure 4, A and E) with immunofluorescence antibodies for NLRP3 (Figure 4, A, D, and E). NLRP3 positivity was significantly elevated in symptomatic dogs compared with normal dogs (Figure 4, A, D, and E). NLRP3 was present within the cellular cytoplasm, as fine granular cytoplasmic labeling

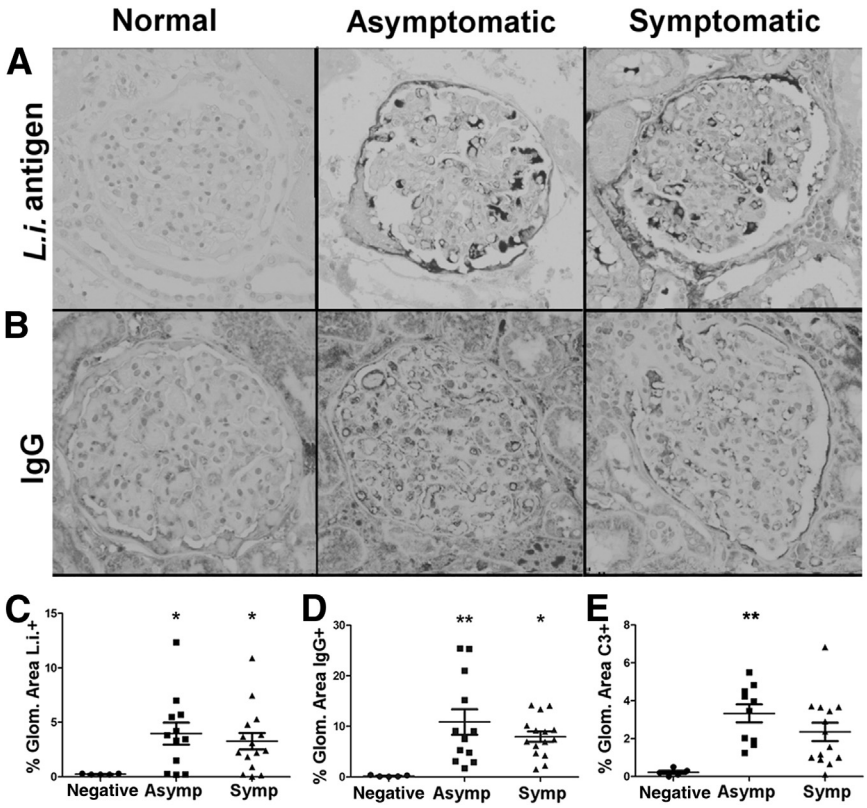

Figure 3 Visceral leishmaniasis (VL)—associated membranoproliferative glomerulonephritis result of *Leishmania infantum* antigen, IgG, and C3 deposition. Formalin-fixed, paraffin-embedded renal cortical sections from *L. infantum*—infected dogs or negative controls evaluated for endocapillary and mesangial deposits of *L. infantum* antigen (**A** and **C**), IgG (**B** and **D**), and complement protein C3 (**E**). **A:** *Leishmania infantum* antigen immunohistochemistry with hematoxylin counterstain. **B:** IgG immunohistochemistry with hematoxylin counterstain. **C:** Percentage glomerular (Glom.) area positive for *L. infantum* antigen in control, asymptomatic (Asymp), and symptomatic (Symp) VL, gated via threshold analysis in ImageJ. **D:** Percentage glomerular area positive for IgG in control, asymptomatic, and symptomatic VL, gated via threshold analysis in ImageJ. **E:** Percentage glomerular area positive for C3 in control, asymptomatic, and symptomatic VL, gated via threshold analysis in ImageJ. **C**—**E:** Statistical analysis was performed via one-way analysis of variance with Tukey post test. Data are given as means ± SEM (**C**—**E**). $^{*}P < 0.05$, $^{**}P < 0.01$. Original magnification, ×400 (**A** and **B**).

near the cell periphery or diffusely throughout the cell cytoplasm, and occasionally within vacuoles. The association between NLRP3 inflammasome induction and the severity of renal disease due to *L. infantum* could be causative or the result of prolonged antigenic and proinflammatory stimulation within the glomerulus.

Autophagy Protein LC3 Is Associated with Symptomatic Infection with *L. infantum*

Macroautophagy is an integral component of organelle and protein recycling within cells, with the most abundant homeostatic macroautophagy in long-lived cells of the body, including neurons, cardiomyocytes, and glomerular podocytes, and within metabolically active cells, such as skeletal muscle and renal tubular epithelium. The importance of macroautophagy in podocyte maintenance of the glomerular filtration apparatus has been previously demonstrated in podocin-conditional LC3 knockout mice.[10] These mice develop protein-losing nephropathy and eventual glomerulosclerosis because of the accumulation of polyubiquitinated protein, with death by 24 weeks of age.[10] In macrophages, the autophagic machinery can also be engaged in response to pathogen-associated molecules, including immune complexes.[24]

To evaluate macroautophagy association with precipitation of VL renal disease and the onset of identifiable MPGN, we labeled formalin-fixed, paraffin-embedded (Figure 4, B and C) or frozen cryosections (Figure 4, A and C) from the renal cortex for LC3 II, then quantified $LC3^{+}$ cells as a percentage of total glomerular cells, from *L. infantum*—negative, asymptomatic, and symptomatic dogs. The percentage of glomerular cells with $LC3^{+}$ puncta was significantly elevated in symptomatic dogs compared with control animals (Figure 4, A—C). Interestingly, LC3 labeling was segmental within glomeruli, consistent with segmental deposits demonstrated by transmission electron microscopy. There was a significant association between presence of $LC3^{+}$ compartments within the glomerulus and severity of MPGN due to *L. infantum*. This could be the result of increased cellular stress and the subsequent recycling of cellular organelles and ubiquitinated proteins, or a direct result of immune complex, complement, and antigen deposition within the glomerular mesangium and subendothelial region of the GBM.

Glomeruli Expressed Increased Inflammasome-Associated ASC during Clinical VL

To further identify roles of autophagy and inflammasomes within glomeruli and closely associated renal tubules during VL, LCM was performed on renal tissue from VL and control dogs. RT-PCR was performed on LCM-acquired renal glomeruli and tubule cells to compare transcription of autophagy-associated genes *Atg7*, *Lc3*, and inflammasome-associated *Pycard* (Asc), *Casp1*, and *Nlrp3* during infection versus control (Figure 5A). Inflammasome-associated Asc transcript up-regulation was observed in *L. infantum*—infected

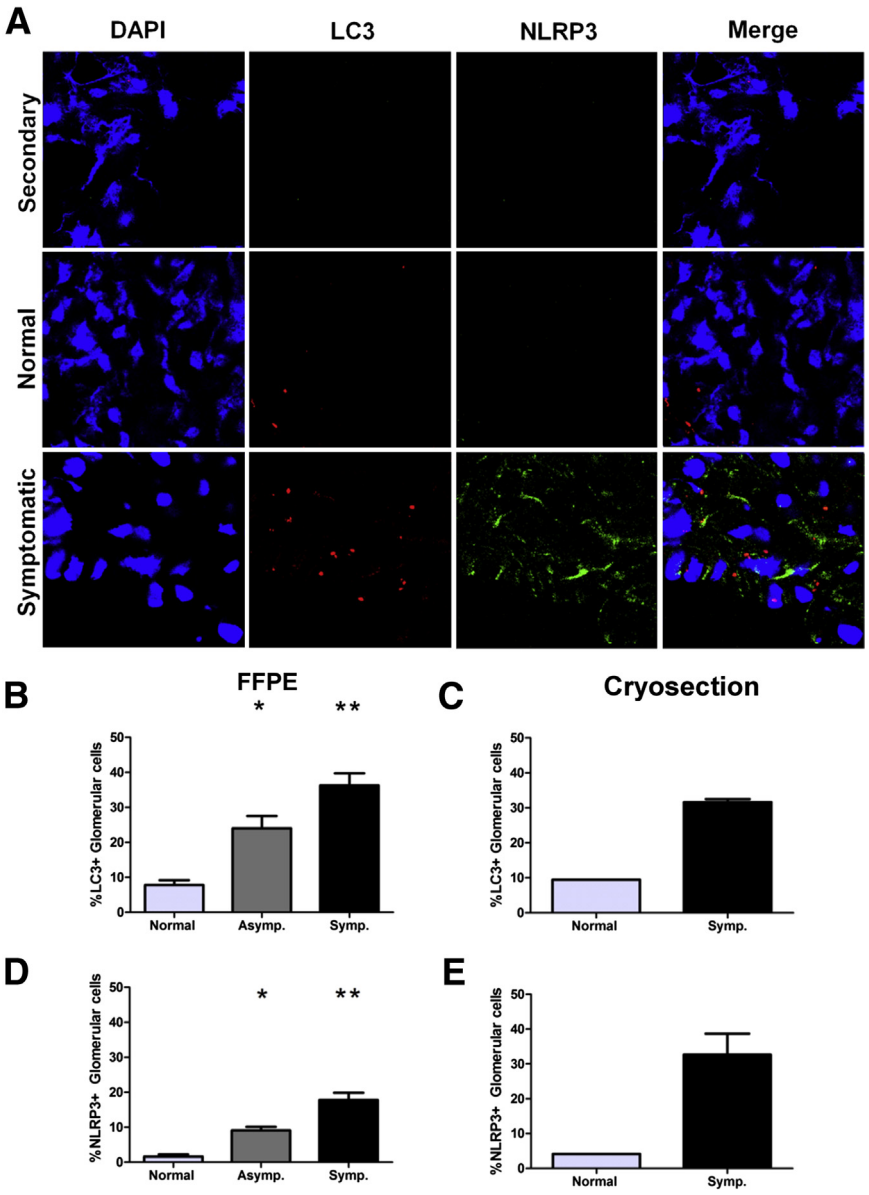

Figure 4 Visceral leishmaniasis (VL)—associated membranoproliferative glomerulonephritis associated with elevated vacuolar-associated light chain 3 (LC3) autophagy protein and nucleotide-binding domain leucine-rich repeat—containing-like receptor family, pyrin domain containing 3 (NLRP3) inflammasomes. Frozen and/or formalin-fixed, paraffin-embedded renal cortical sections labeled with immunofluorescence antibodies, imaged, and counted via confocal microscopy evaluated presence of LC3-positive autophagy-associated vacuoles and presence of NLRP3-positive inflammasomes. **A:** Immunofluorescence of renal glomeruli with antibody control sample (**top panels**), *Leishmania infantum*—negative dogs (**middle panels**), and dogs with symptomatic VL (**bottom panels**). Cells stained with DAPI and labeled for NLRP3 and LC3. **B** and **C:** Percentage LC3-positive cells from total nucleated glomerular cells in *L. infantum*—negative, asymptomatic (Asymp.), and symptomatic (Symp.) dogs. **D** and **E:** Percentage NLRP3-positive cells from total glomerular cells of *L. infantum*—negative, asymptomatic, and symptomatic dogs. Data were analyzed via one-way analysis of variance with Tukey post test for significance. $*P < 0.05$, $**P < 0.01$.

dog glomeruli and tubules relative to control animals ($P = 0.03230$ and $P = 0.0014$, respectively). Autophagy-associated *Atg7* and *Lc3* were up-regulated in VL dog tubules ($P = 0.0189$ and $P = 0.0269$, respectively) compared with control dogs. Macroautophagy- and inflammasome-associated genes were up-regulated in canine renal tissue during clinical VL. To more specifically evaluate the contribution of ASC to *L. infantum*—associated glomerulonephritis, $Asc^{-/-}$ mice infected with 10^6 *L. infantum* parasites were evaluated for ultrastructural lesions at 4 weeks after infection. In mice with significant parasite infection at 4 weeks, ultrastructural lesions observed during *L. infantum* infection in both $Asc^{-/-}$ and WT mice were mild podocyte effacement with blunting and fusion of foot processes (Figure 5B) and podocyte hypertrophy with the GBM (Figure 5C) compared with uninfected controls. Podocytes from *L. infantum*—infected $Asc^{-/-}$ mice had numerous intracellular multivesicular bodies (Figure 5C), which were not present in uninfected controls and rare in WT *L. infantum*—infected mice.

Inflammasome Complex Is Up-Regulated and Activated in Kidneys Isolated from *L. Infantum*—Infected Dogs Compared with Uninfected Control Dogs

The inflammasome is a multiprotein complex. ASC is an adaptor protein, whereas NLRP3 protein is the scaffolding structure. These proteins were assayed in kidney lysates isolated from *L. infantum*—infected dogs. ASC was significantly up-regulated in samples isolated from infected dogs compared with controls (Figure 6A). Similarly, NLRP3 protein was up-regulated in kidney lysates isolated

from infected dogs compared with controls (Figure 6B). Because the inflammasome complex represents one way by which pro−IL-1β can be activated via cleavage events to become active IL-1β, it is likely that this is the main pathway in the kidneys from *L. infantum*−infected dogs to produce this inflammatory cytokine.[35] Indeed, there is increased IL-1β in samples isolated from *L. infantum*−infected dogs of both the pro− and active IL-1β forms (Figure 6C). Although increased levels of IL-1β were detected locally in the kidney, no difference in circulating IL-1β from serum samples collected from *L. infantum*−infected dogs compared with control was observed (Supplemental Figure S1).

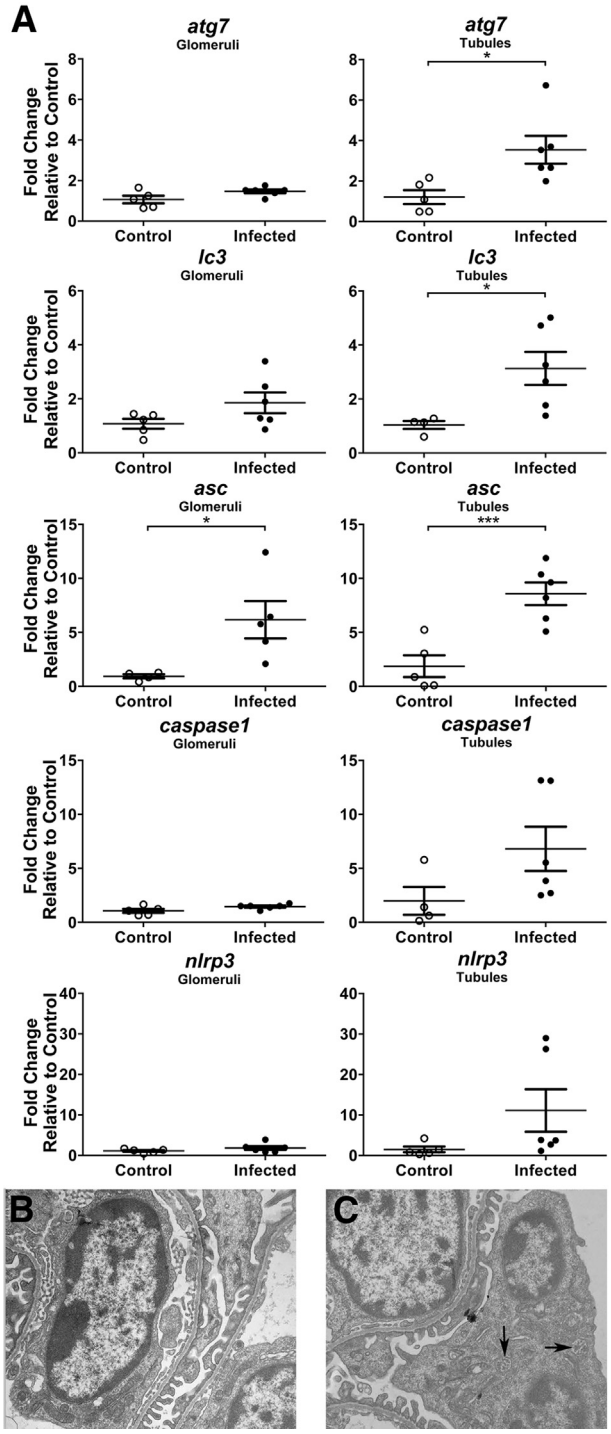

Figure 5 Glomeruli and tubules from visceral leishmaniasis−infected dogs express higher levels of autophagy and inflammasome-associated genes. **A:** Laser-capture microdissected glomeruli and tubules analyzed for RNA transcription by RT-PCR. Analysis of Atg7, Lc3, Asc, caspase1, and NLRP3 relative to average C_T value of healthy control cells via SYBR Green (Life Technologies, Grand Island, NY). *GAPDH* was used as endogenous control reference gene. **B** and **C:** Apoptosis-associated speck-like protein containing a caspase activation and recruitment domain $(Asc)^{-/-}$ mice infected 4 weeks with 10^6 metacyclic *Leishmania infantum* promastigotes. **B:** Both wild-type and $Asc^{-/-}$ glomeruli develop mild podocyte foot process blunting and fusion compared with uninfected controls. Transmission electron microscopy (TEM) was used. **C:** $Asc^{-/-}$ mice have increased multivesicular bodies (**arrows**) within hypertrophied podocytes. TEM was used. Representative of ultrastructural glomerular lesions from three infected $Asc^{-/-}$ mice and three WT infected mice. Data are given as means ± SEM (**A**). $n = 5$ per group (**A**). $^*P < 0.05$, $^{***}P < 0.001$. Original magnification, ×13,000 (**B** and **C**).

Discussion

Renal disease is a complication of VL in human and canine patients. Nearly 100% of clinically affected dogs have renal lesions. Renal pathology is present in approximately 30% of human VL patients, with a rate of acute kidney injury in children of approximately 25% to 45.9%.[1−4,36−38] VL renal lesions were previously characterized as progressive glomerulonephritis, including mesangial proliferative, membranoproliferative, focal-segmental, and minimal-change glomerulonephritis, and in a small percentage, crescentic glomerulonephritis.[2,5,7,29] These widely differing morphological classifications may be because of differences in chronicity of glomerular injury, but have little correlation with type of glomerular insult or glomerular response to insult. The recent expanded World Health Organization classification includes molecular characterization of glomerular deposits in addition to routine histological evaluation and electron microscopy.[8] This proposed classification provides improved guidance and may elucidate molecular targets for therapy to reduce long-term renal insufficiency and ESRD.

Dogs with symptomatic VL typically have hypergammaglobulinemia and abundant circulating parasite antigen.[22] Previous studies evaluating proteins associated with VL glomerular deposits had conflicting results.[7,30] One study found granular deposits of IgG, IgM, and C3 within 31 of 34 dogs examined.[30] A similar study identified no difference in the degree of IgG, IgM, or C3 deposits between infected and control dogs.[7] The latter study characterized a significant increase in *L. infantum* antigen and inflammatory cells within the GBM and mesangium.[7] We primarily found renal pathology consisting of type I MPGN, associated with segmental subendothelial and mesangial deposits of *L. infantum* antigen, IgG, and complement protein C3 (Table 2 and Figures 1−3).

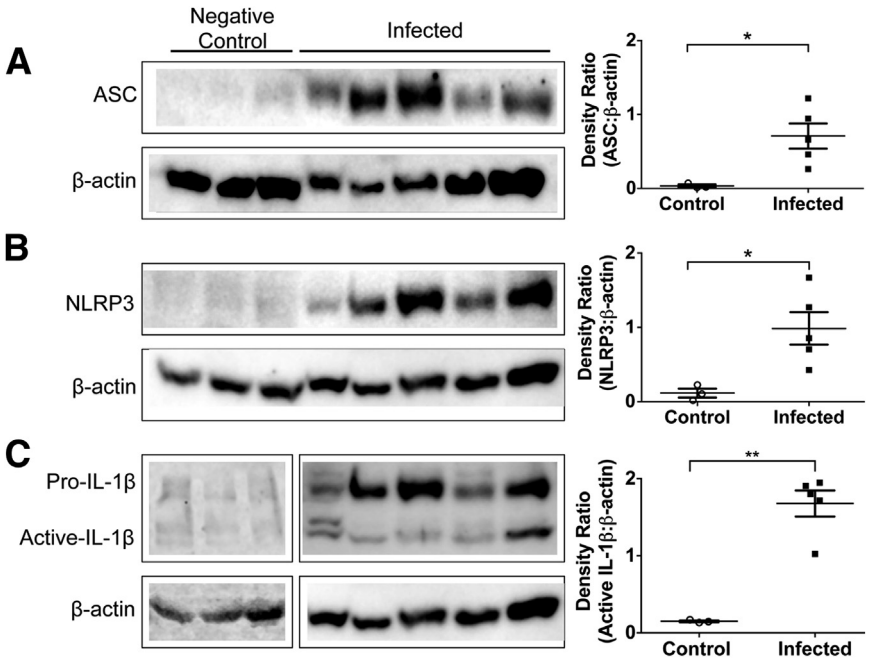

Figure 6 Inflammasome proteins are increased in *Leishmania infantum*—infected dogs compared with uninfected controls, although intracellular IL-1β is decreased. Kidney protein lysates or peripheral blood mononuclear cells (5 μg) were electrophoresed and transferred to polyvinylidene difluoride (PVDF) for protein-target identification. PDVF was probed for apoptosis-associated speck-like protein containing a caspase activation and recruitment domain (ASC; **A**), nucleotide-binding domain leucine-rich repeat—containing-like receptor family, pyrin domain containing 3 (NLRP3; **B**), and IL-1β (**C**); membranes were stripped and reprobed for β-actin as loading control (**A** and **B**). Bands were digitally imaged, and photon densitometry was calculated for band semiquantification as a ratio to β-actin. Statistical analysis was performed with *t*-test with Welsh correction. Data are given as means ± SEM (**A**—**C**). $n = 3$ (control); $n = 5$ (infected). $^{*}P < 0.05$, $^{**}P < 0.01$.

Disparities between studies could be because of stage and severity of disease in each cohort. Our study was both a prospective US dog sample from 2007 to 2012 and Brazilian dogs sampled in 2011. Animals in the US cohort, although symptomatic, may have been identified and euthanized at earlier stages of disease than dogs from Brazil in the current and in previous studies, before severe fibrosis and glomerulosclerosis.[1,2,7,28] US dogs were more likely to have undergone pharmacological therapy than Brazilian dogs used in this study. These differences in disease severity have impact on the type and density of deposits present and morphological characteristics within glomerular lesions.

Our study used VL-associated glomerulonephritis to identify relationships between macroautophagy marker LC3, NLRP3, symptomatic disease, and severity of glomerular lesions. $LC3^{+}$ autophagic puncta and NLRP3 protein expression were significantly increased in glomeruli during asymptomatic and symptomatic VL compared with controls (Figure 4). Macroautophagy in response to glomerular immune complex deposition may be a major mechanism for removal of accumulated proteins, complement, and immune complexes from the GBM and mesangium. NLRP3 activation in response to immune complex deposition is a possible source for increased IL-1β and IL-18 within the kidney, with important chemotactic and proinflammatory roles, correlated with inflammatory renal disease and renal reperfusion injury after ischemia.[19] Janczy et al[39] demonstrated immune complex—mediated inhibition of IL-1β secretion and inflammasome activation, differing from the results from the current study. However, in this study, immune complex—mediated suppression of IL-1β secretion was evident only if immune complexes were added before the inflammasome agonist during priming. In contrast, interpretation of MPGN during chronic naturally occurring leishmaniasis must consider the context of the concurrent local and systemic immune response to the infection. First, infection is chronic, with gradual disease progression over months to years, far removed from an acute challenge. Second, kidneys from *Leishmania*-infected dogs contain moderate to marked infiltrates of macrophages in addition to aggregates of lymphocytes and plasma cells, which contribute to the cytokine profile of the kidney and likely effect phenotypic responses of native cell types. Multiple studies characterize renal tubular cell secretion of IL-1β and IL-18 in response to tubulointerstitial inflammation, driving inflammation.[19,40,41] Mouse studies evaluating glomerular NLRP3 activation had conflicting results. A single study of NLRP3 inflammasome activation during mouse anti-GBM disease found low expression of NLRP3, caspase-1, and pro—IL-1β mRNA and found glomeruli incapable of producing NLRP3, caspase-1, and IL-1β. In two other murine studies, NLRP3 was expressed by glomerular podocytes with NADPH oxidase—induced NLRP3 inflammasome activation, driving caspase-1 activity and triggering podocyte injury.[20]

During infection, autophagosomes targeted microbial products to pattern recognition receptor—bearing compartments (xenophagy), and facilitated antigen presentation via major histocompatibility complex II.[42] Noncanonical autophagy (or LC3-associated phagocytosis) proceeds in the absence of canonical pathway proteins Unc-51-like kinase-1 and focal adhesion kinase family interacting protein of 200 kD in response to stimulation through phosphatidylinositol 3-kinase and dependent on autophagy complex proteins Beclin 1, ATG5, and ATG7.[43—45] This pathway was initiated in response to Fc-γ receptor engagement by immune complexes, and stimulated NADPH oxidase production in macrophages.[24]

The formation of LC3-II from LC3-I into its autophagosomal membrane–associated form resulted in discrete puncta, indicative of autophagosome formation.[46] A previous study correlated presence of increased autophagosomes with IgA nephropathy patients, and multiple studies evaluated the role of autophagy in glomerular homeostasis.[10,11,13,47] In this study, we demonstrated association of renal lesions, disease severity, and elevated glomerular LC3-II and expression of tubular ATG7 in infectious disease–related MPGN (Figures 4 and 5). Our findings elucidate a potential role for glomerular autophagy in response to immune complex deposition within the glomerulus.

Previous studies demonstrated significant cross talk between inflammasome and autophagy pathways. ASC and NLRP3 were shown to drive the secretion of major histocompatibility complex II–bearing exosomes from autophagolysosomes, in the form of multivesicular bodies in microglia, macrophages, and dendritic cells independent of caspase 1.[48,49] Our observed accumulation of multivesicular bodies in podocytes of infected $Asc^{-/-}$ mice (Figure 5C), not uncommonly identified in diagnostic renal biopsy specimens, could be associated with a similar secretion of multivesicular exosomes from autophagosomes. Additional experiments via model systems may further elucidate the necessity and sufficiency of autophagy and inflammasome mechanisms in VL-associated MPGN.

Under chronic inflammatory conditions, including diabetic nephropathy, renal nonmyeloid cells were contributing factors to NLRP3 inflammasome activation and inflammation.[50] In the context of *Leishmania*-induced glomerulonephritis, it is plausible that many nonmyeloid cells contribute to inflammatory conditions, leading to renal disease. NLRP3 and caspase-1 were not up-regulated in canine VL renal tissue; however, ASC was significantly up-regulated in both glomeruli and tubules in these animals. Although commonly found with NLRP3, ASC was shown to act independently of the NLRP3-inflammasome recruitment to produce inflammatory cytokines. During *Borrelia*-associated arthritis, IL-1β production was dependent on ASC/caspase-1 interaction but did not depend on NLRP3 recruitment.[51] ASC is known to interact with the protein absent in melanoma 2,[52,53] and perhaps this alternative pathway is related to the VL-inflammatory response within renal glomeruli. Alternatively, NLRP3 basal expression is sufficient to produce mature IL-1β.[54] An additional possibility is that ASC serves as an adapter protein for signaling pathways independent of NLRP3, specific to glomerular podocytes and mesangial cells.

Our data indicate that the inflammasome complex is being up-regulated and activated in the kidney of *L. infantum*–infected dogs. More important, ASC and NLRP3 proteins were increased in lysates generated from *L. infantum*–infected dogs compared with controls (Figure 6). This dramatic increase was not wholly observed at the transcriptional level because the inflammasome is tightly regulated post-transcriptionally (Figure 5). It is likely that mechanisms outside of gene transcription are regulating NLRP3 multimeric assembly and activation. Likewise, cellular infiltrate may be contributing to additional inflammasome components not observed by LCM-generated cDNA and is being resolved with Western-based protein analysis.

IL-1β was present in kidney lysates and *L. infantum*–infected dogs (Figure 6C). Pro–IL-1β undergoes post-translational modification to become activated and subsequently secreted.[55] Interestingly, we observed both the proform of IL-1β present in kidney lysates from infected dogs and active IL-1β, indicating that IL-1β processing had occurred (Figure 6C).

Strong associations presented within this naturally occurring model of MPGN suggest a role for glomerular inflammasome activation and autophagy in either the induction of or response to glomerular deposition of immune complexes and antigen. Therapeutic targeting of these molecules may have potential to limit long-term renal damage during MPGN.

Acknowledgments

We thank Judith Stasko (Agriculture Research Service National Animal Disease Center) for assistance with processing and capture of electron microscopic data; the Iowa State University Histopathology Laboratory for technical expertise and assistance; Deborah Moore, Diane Gerjets, Socorro Medeiros, and Jack Gallup for technical assistance; Drs. Katherine Gibson-Corley and Mary Wilson for their contributions to this study; and Dr. James Martins for his help in providing renal tissue samples for comparative controls in RT-PCR.

Supplemental Data

Supplemental material for this article can be found at *http://dx.doi.org/10.1016/j.ajpath.2015.04.017*.

References

1. Benderitter T, Casanova P, Nashkidachvili L, Quilici M: Glomerulonephritis in dogs with canine leishmaniasis. Ann Trop Med Parasitol 1988, 82:335–341
2. Costa FA, Goto H, Saldanha LC, Silva SM, Sinhorini IL, Silva TC, Guerra JL: Histopathologic patterns of nephropathy in naturally acquired canine visceral leishmaniasis. Vet Pathol 2003, 40:677–684
3. Dutra M, Martinelli R, de Carvalho EM, Rodrigues LE, Brito E, Rocha H: Renal involvement in visceral leishmaniasis. Am J Kidney Dis 1985, 6:22–27
4. Liborio AB, Rocha NA, Oliveira MJ, Franco LF, Aguiar GB, Pimentel RS, Abreu KL, Silva GB Jr, Daher EF: Acute kidney injury in children with visceral leishmaniasis. Pediatr Infect Dis J 2012, 31:451–454
5. Sayari M, Avizeh R, Barati F: Microscopic evaluation of renal changes in experimental canine visceral leishmaniosis after chemo- and immunotherapy. Pak J Biol Sci 2008, 11:1630–1633

6. Beltrame A, Arzese A, Camporese A, Rorato G, Crapis M, Tarabini-Castellani G, Boscutti G, Pizzolitto S, Calianno G, Matteelli A, Di Muccio T, Gramiccia M, Viale P: Acute renal failure due to visceral leishmaniasis by Leishmania infantum successfully treated with a single high dose of liposomal amphotericin B. J Travel Med 2008, 15: 358–360
7. Costa FA, Prianti MG, Silva TC, Silva SM, Guerra JL, Goto H: T cells, adhesion molecules and modulation of apoptosis in visceral leishmaniasis glomerulonephritis. BMC Infect Dis 2010, 10:112
8. Bomback AS, Appel GB: Pathogenesis of the C3 glomerulopathies and reclassification of MPGN. Nat Rev Nephrol 2012, 8:634–642
9. Sethi S, Fervenza FC: Membranoproliferative glomerulonephritis: a new look at an old entity. N Engl J Med 2012, 366: 1119–1131
10. Hartleben B, Godel M, Meyer-Schwesinger C, Liu S, Ulrich T, Kobler S, Wiech T, Grahammer F, Arnold SJ, Lindenmeyer MT, Cohen CD, Pavenstadt H, Kerjaschki D, Mizushima N, Shaw AS, Walz G, Huber TB: Autophagy influences glomerular disease susceptibility and maintains podocyte homeostasis in aging mice. J Clin Invest 2010, 120:1084–1096
11. Sato S, Yanagihara T, Ghazizadeh M, Ishizaki M, Adachi A, Sasaki Y, Igarashi T, Fukunaga Y: Correlation of autophagy type in podocytes with histopathological diagnosis of IgA nephropathy. Pathobiology 2009, 76:221–226
12. Sato S, Adachi A, Sasaki Y, Dai W: Autophagy by podocytes in renal biopsy specimens. J Nippon Med Sch 2006, 73:52–53
13. Sato S, Kitamura H, Adachi A, Sasaki Y, Ghazizadeh M: Two types of autophagy in the podocytes in renal biopsy specimens: ultrastructural study. J Submicrosc Cytol Pathol 2006, 38: 167–174
14. Ma T, Zhu J, Chen X, Zha D, Singhal PC, Ding G: High glucose induces autophagy in podocytes. Exp Cell Res 2013, 319:779–789
15. Chevrier M, Brakch N, Celine L, Genty D, Ramdani Y, Moll S, Djavaheri-Mergny M, Brasse-Lagnel C, Annie Laquerriere AL, Barbey F, Bekri S: Autophagosome maturation is impaired in Fabry disease. Autophagy 2010, 6:589–599
16. Strowig T, Henao-Mejia J, Elinav E, Flavell R: Inflammasomes in health and disease. Nature 2012, 481:278–286
17. Sutterwala FS, Haasken S, Cassel SL: Mechanism of NLRP3 inflammasome activation. Ann N Y Acad Sci 2014, 1319:82–95
18. Clay GM, Sutterwala FS, Wilson ME: NLR proteins and parasitic disease. Immunol Res 2014, 59:142–152
19. Anders HJ, Muruve DA: The inflammasomes in kidney disease. J Am Soc Nephrol 2011, 22:1007–1018
20. Abais JM, Zhang C, Xia M, Liu Q, Gehr TW, Boini KM, Li PL: NADPH oxidase-mediated triggering of inflammasome activation in mouse podocytes and glomeruli during hyperhomocysteinemia. Antioxid Redox Signal 2013, 18:1537–1548
21. Boini KM, Xia M, Abais JM, Li G, Pitzer AL, Gehr TW, Zhang Y, Li PL: Activation of inflammasomes in podocyte injury of mice on the high fat diet: effects of ASC gene deletion and silencing. Biochim Biophys Acta 2014, 1843:836–845
22. Boggiatto PM, Ramer-Tait AE, Metz K, Kramer EE, Gibson-Corley K, Mullin K, Hostetter JM, Gallup JM, Jones DE, Petersen CA: Immunologic indicators of clinical progression during canine Leishmania infantum infection. Clin Vaccine Immunol 2010, 17:267–273
23. Gibson-Corley KN, Hostetter JM, Hostetter SJ, Mullin K, Ramer-Tait AE, Boggiatto PM, Petersen CA: Disseminated Leishmania infantum infection in two sibling foxhounds due to possible vertical transmission. Can Vet J 2008, 49:1005–1008
24. Henault J, Martinez J, Riggs JM, Tian J, Mehta P, Clarke L, Sasai M, Latz E, Brinkmann MM, Iwasaki A, Coyle AJ, Kolbeck R, Green DR, Sanjuan MA: Noncanonical autophagy is required for type I interferon secretion in response to DNA-immune complexes. Immunity 2012, 37:986–997
25. Coussens G, Aesaert S, Verelst W, Demeulenaere M, De Buck S, Njuguna E, Inzé D, Van Lijsebettens M: Brachypodium distachyon promoters as efficient building blocks for transgenic research in maize. J Exp Bot 2012, 63:4263–4273
26. Livak KJ, Schmittgen TD: Analysis of relative gene expression data using real-time quantitative PCR and the 2(-Delta Delta C(T)) Method. Methods 2001, 25:402–408
27. Maeda S, Ohno K, Uchida K, Nakashima K, Fukushima K, Tsukamoto A, Nakajima M, Fujino Y, Tsujimoto H: Decreased immunoglobulin A concentrations in feces, duodenum, and peripheral blood mononuclear cells of dogs with inflammatory bowel disease. J Vet Intern Med 2013, 27:47–55
28. Sow FB, Gallup JM, Sacco RE, Ackermann MR: Laser capture microdissection revisited as a tool for transcriptomic analysis: application of an Excel-based qPCR preparation software (PREXCEL-Q). Int J Biomed Sci 2009, 5:105–124
29. Poli A, Abramo F, Mancianti F, Nigro M, Pieri S, Bionda A: Renal involvement in canine leishmaniasis: a light-microscopic, immunohistochemical and electron-microscopic study. Nephron 1991, 57: 444–452
30. Nieto CG, Navarrete I, Habela MA, Serrano F, Redondo E: Pathological changes in kidneys of dogs with natural Leishmania infection. Vet Parasitol 1992, 45:33–47
31. Lopez-Hernandez FJ, Lopez-Novoa JM: Role of TGF-beta in chronic kidney disease: an integration of tubular, glomerular and vascular effects. Cell Tissue Res 2012, 347:141–154
32. Dostert C, Petrilli V, Van Bruggen R, Steele C, Mossman BT, Tschopp J: Innate immune activation through Nalp3 inflammasome sensing of asbestos and silica. Science 2008, 320:674–677
33. Martinon F, Petrilli V, Mayor A, Tardivel A, Tschopp J: Gout-associated uric acid crystals activate the NALP3 inflammasome. Nature 2006, 440:237–241
34. Chen K, Zhang J, Zhang W, Zhang J, Yang J, Li K, He Y: ATP-P2X4 signaling mediates NLRP3 inflammasome activation: a novel pathway of diabetic nephropathy. Int J Biochem Cell Biol 2013, 45: 932–943
35. Rodgers MA, Bowman JW, Liang Q, Jung JU: Regulation where autophagy intersects the inflammasome. Antioxid Redox Signal 2014, 20:495–506
36. DEB T, Hoshino-Shimizu S, Neto VA, Duarte IS, Penna DO: Glomerular involvement in human kala-azar: a light, immunofluorescent, and electron microscopic study based on kidney biopsies. Am J Trop Med Hyg 1975, 24:9–18
37. Zatelli A, Borgarelli M, Santilli R, Bonfanti U, Nigrisoli E, Zanatta R, Tarducci A, Guarraci A: Glomerular lesions in dogs infected with Leishmania organisms. Am J Vet Res 2003, 64:558–561
38. Rocha NA, Silva GB, Oliveira MJ, Abreu KL, Franco LF, Silva MP, Garcia AV, Daher EF: Visceral leishmaniasis in children: a cohort of 120 patients in a metropolitan city of Brazil. Turk J Pediatr 2011, 53: 154–160
39. Janczy JR, Ciraci C, Haasken S, Iwakura Y, Olivier AK, Cassel SL, Sutterwala FS: Immune complexes inhibit IL-1 secretion and inflammasome activation. J Immunol 2014, 193:5190–5198
40. Vilaysane A, Chun J, Seamone ME, Wang W, Chin R, Hirota S, Li Y, Clark SA, Tschopp J, Trpkov K, Hemmelgarn BR, Beck PL, Muruve DA: The NLRP3 inflammasome promotes renal inflammation and contributes to CKD. J Am Soc Nephrol 2010, 21: 1732–1744
41. Timoshanko JR, Kitching AR, Iwakura Y, Holdsworth SR, Tipping PG: Contributions of IL-1beta and IL-1alpha to crescentic glomerulonephritis in mice. J Am Soc Nephrol 2004, 15:910–918
42. Munz C: Antigen processing for MHC class II presentation via autophagy. Front Immunol 2012, 3:9
43. Sanjuan MA, Dillon CP, Tait SW, Moshiach S, Dorsey F, Connell S, Komatsu M, Tanaka K, Cleveland JL, Withoff S, Green DR: Toll-like receptor signalling in macrophages links the autophagy pathway to phagocytosis. Nature 2007, 450:1253–1257

44. Martinez J, Almendinger J, Oberst A, Ness R, Dillon CP, Fitzgerald P, Hengartner MO, Green DR: Microtubule-associated protein 1 light chain 3 alpha (LC3)-associated phagocytosis is required for the efficient clearance of dead cells. Proc Natl Acad Sci U S A 2011, 108:17396−17401
45. Florey O, Kim SE, Sandoval CP, Haynes CM, Overholtzer M: Autophagy machinery mediates macroendocytic processing and entotic cell death by targeting single membranes. Nat Cell Biol 2011, 13:1335−1343
46. Choi AM, Ryter SW, Levine B: Autophagy in human health and disease. N Engl J Med 2013, 368:651−662
47. Kim SI, Na HJ, Ding Y, Wang Z, Lee SJ, Choi ME: Autophagy promotes intracellular degradation of type I collagen induced by transforming growth factor (TGF)-beta1. J Biol Chem 2012, 287: 11677−11688
48. Quinnell RJ, Courtenay O: Transmission, reservoir hosts and control of zoonotic visceral leishmaniasis. Parasitology 2009, 136:1915−1934
49. Takenouchi T, Nakai M, Iwamaru Y, Sugama S, Tsukimoto M, Fujita M, Wei J, Sekigawa A, Sato M, Kojima S, Kitani H, Hashimoto M: The activation of P2X7 receptor impairs lysosomal functions and stimulates the release of autophagolysosomes in microglial cells. J Immunol 2009, 182:2051−2062
50. Shahzad K, Bock F, Dong W, Wang H, Kopf S, Kohli S, Al-Dabet MM, Ranjan S, Wolter J, Wacker C, Biemann R, Stoyanov S, Reymann K, Soderkvist P, Gross O, Schwenger V, Pahernik S, Nawroth PP, Grone HJ, Madhusudhan T, Isermann B: Nlrp3-inflammasome activation in non-myeloid-derived cells aggravates diabetic nephropathy. Kidney Int 2015, 87:74−84
51. Oosting M, Buffen K, Malireddi SR, Sturm P, Verschueren I, Koenders MI, van de Veerdonk FL, van der Meer JW, Netea MG, Kanneganti TD, Joosten LA: Murine Borrelia arthritis is highly dependent on ASC and caspase-1, but independent of NLRP3. Arthritis Res Ther 2012, 14:R247
52. Tsuchiya K, Hara H: The inflammasome and its regulation. Crit Rev Immunol 2014, 34:41−80
53. Hara H, Tsuchiya K, Kawamura I, Fang R, Hernandez-Cuellar E, Shen Y, Mizuguchi J, Schweighoffer E, Tybulewicz V: Phosphorylation of the adaptor ASC acts as a molecular switch that controls the formation of speck-like aggregates and inflammasome activity. Nat Immunol 2013, 14:1247−1255
54. Guarda G, Zenger M, Yazdi AS, Schroder K, Ferrero I, Menu P, Tardivel A, Mattmann C, Tschopp J: Differential expression of NLRP3 among hematopoietic cells. J Immunol 2011, 186:2529−2534
55. Negash AA, Ramos HJ, Crochet N, Lau DT, Doehle B, Papic N, Delker DA, Jo J, Bertoletti A, Hagedorn CH, Gale M Jr: IL-1beta production through the NLRP3 inflammasome by hepatic macrophages links hepatitis C virus infection with liver inflammation and disease. PLoS Pathog 2013, 9:e1003330